Cell Reports

Article

# Hippocampal Interneuronal α7 nAChRs Modulate Theta Oscillations in Freely Moving Mice

## Graphical Abstract

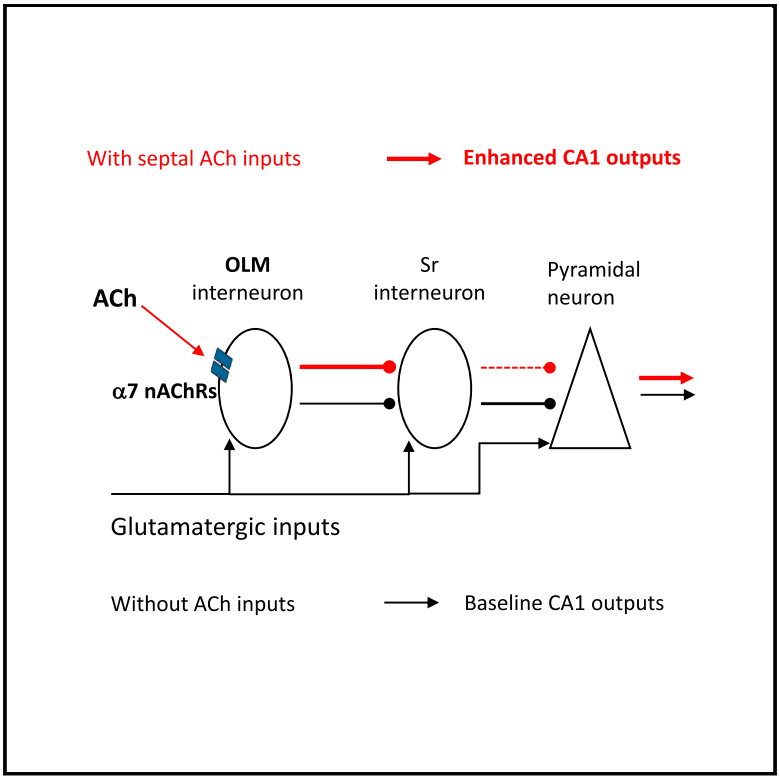


## Authors

Zhenglin Gu, Kathleen G. Smith, Georgia M. Alexander, ..., Boris Gutkin, Patricia Jensen, Jerrel L. Yakel

## Correspondence

yakel@niehs.nih.gov

## In Brief

Gu et al. observe that hippocampal α7-nAChR antagonist infusion reduces theta power and impairs Y-maze spontaneous alternation performance in freely moving mice. They further find that α7 nAChRs expressed in interneurons are critical for this regulation, revealing a potential mechanism underlying nicotinic regulation of hippocampal functions.

## Highlights

- Hippocampal α7 nAChRs regulate theta power in freely moving mice
- Hippocampal α7 nAChRs regulate Y-maze spontaneous alternation performance
- Interneuronal α7 nAChRs are critical for theta and Y-maze regulation

Gu et al., 2020, Cell Reports *31*, 107740
June 9, 2020 
https://doi.org/10.1016/j.celrep.2020.107740

CellPress

Cell Reports

CellPress
OPEN ACCESS

Article

# Hippocampal Interneuronal α7 nAChRs Modulate Theta Oscillations in Freely Moving Mice

Zhenglin Gu,[1] Kathleen G. Smith,[1] Georgia M. Alexander,[1] Inês Guerreiro,[2] Serena M. Dudek,[1] Boris Gutkin,[2,3] Patricia Jensen,[1] and Jerrel L. Yakel[1,4,*]

[1]Neurobiology Laboratory, National Institute of Environmental Health Sciences, National Institutes of Health, Department of Health and Human Services, Research Triangle Park, NC 27709, USA

[2]Group for Neural Theory, LNC INSERM U960, DEC Ecole Normale Superieure PSL University, Paris 75005, France

[3]Center for Cognition and Decision Making, Institute for Cognitive Neuroscience, NRU Higher School of Economics, Moscow 101000, Russia

[4]Lead Contact

*Correspondence: yakel@niehs.nih.gov

https://doi.org/10.1016/j.celrep.2020.107740

## SUMMARY

Muscarinic acetylcholine receptors (mAChRs) are critically involved in hippocampal theta generation, but much less is known about the role of nicotinic AChRs (nAChRs). Here we provide evidence that α7 nAChRs expressed on interneurons, particularly those in *oriens lacunosum moleculare* (OLM), also regulate hippocampal theta generation. Local hippocampal infusion of a selective α7 nAChR antagonist significantly reduces hippocampal theta power and impairs Y-maze spontaneous alternation performance in freely moving mice. By knocking out receptors in different neuronal subpopulations, we find that α7 nAChRs expressed in OLM interneurons regulate theta generation. Our *in vitro* slice studies indicate that α7 nAChR activation increases OLM neuron activity that, in turn, enhances pyramidal cell excitatory postsynaptic currents (EPSCs). Our study also suggests that mAChR activation promotes transient theta generation, while α7 nAChR activation facilitates future theta generation by similar stimulations, revealing a complex mechanism whereby cholinergic signaling modulates different aspects of hippocampal theta oscillations through different receptor subtypes.

## INTRODUCTION

Theta oscillations are large, synchronized neuronal activities observed in the hippocampus and many hippocampus-associated brain regions during active exploration and many other behaviors. These oscillations are believed to play an important role in higher cognitive functions such as spatial learning and memory (Battaglia et al., 2011; Buzsáki, 2002, 2005; Buzsáki and Moser, 2013; Hasselmo, 2005; Winson, 1978). The mechanisms underlying theta generation are still not fully understood, likely because of the complex nature of theta generation that involves multiple brain regions and several different neurotransmitter systems (Buzsáki, 2002; Stewart and Fox, 1990). Theta oscillations closely correlate with a variety of behavioral states such as movement, spatial learning and memory, arousal, and anxiety (Korotkova et al., 2018). The theta frequency can be modulated or modified by many factors including novel environment (Jeewajee et al., 2008b; Wells et al., 2013), locomotor speed (Jeewajee et al., 2008a; Wells et al., 2013; Whishaw and Vanderwolf, 1973), and movement onset and acceleration (Bush et al., 2017). The septal neurons are thought to be the major pacemakers of theta oscillations (Gogolák et al., 1968; Green and Arduini, 1954; Petsche et al., 1968; Stewart and Fox, 1990; Stumpf et al., 1962), although other brain regions such as the hippocampus may also be capable of independently generating theta oscillations (Goutagny et al., 2009). Two neurotransmitter receptor classes—muscarinic ACh receptors (mAChRs) and the NMDA subtype of glutamate receptors—are strongly implicated in theta generation. The mAChRs are the major mediator of type-II theta oscillations, which have a frequency of 4–9 Hz and often occur during alert immobility or under urethane anesthesia in rodents (Buzsáki, 2002; Kramis et al., 1975; Sainsbury et al., 1987). Septal neurons (Lawson and Bland, 1993; Monmaur et al., 1993; Monmaur and Breton, 1991), especially parvalbumin-positive interneurons (Dannenberg et al., 2015), are critical in type-II theta generation. In contrast, NMDA receptors are important for type-I theta oscillations, which have a higher frequency of 6–12 Hz and mainly occur during active exploration (Buzsáki, 2002; Leung and Shen, 2004; Leung and Desborough, 1988). Likely, type-I and type-II theta share some common mechanisms of generation, as type-I theta has both atropine-sensitive and atropine-resistant components (Kramis et al., 1975; Lee et al., 1994; Vanderwolf and Baker, 1986; Vanderwolf et al., 1985). In addition, septal cholinergic lesions have been shown to not only eliminate atropine-sensitive type-II theta oscillations under urethane anesthesia, but also severely impair type-I theta oscillations in freely moving animals (Lee et al., 1994; Yoder and Pang, 2005). However, the cholinergic receptor subtypes and their locations involved in type-I theta generation in freely moving animals are less clear.

Please cite this article in press as: Gu et al., Hippocampal Interneuronal α7 nAChRs Modulate Theta Oscillations in Freely Moving Mice, Cell Reports (2020), https://doi.org/10.1016/j.celrep.2020.107740



Our recent study suggested that hippocampal mAChRs, especially the M1 subtype of receptors expressed on pyramidal neurons, contributed to hippocampal theta generation in freely running mice (Gu et al., 2017). However, the finding that septal cholinergic lesions resulted in greater theta power reduction than after atropine treatment suggests that in addition to mAChRs, nicotinic ACh receptors (nAChRs) may also be playing a role in theta generation in freely moving animals (Buzsáki, 2002; Lee et al., 1994). nAChRs are highly expressed in the hippocampus (Martin and Aceto, 1981) and modulate higher brain cognitive functions such as learning and memory (Kenney and Gould, 2008; Levin and Simon, 1998). In the hippocampus, the majority of nAChRs are α7-subunit-containing nAChRs (α7 nAChRs), which have high calcium permeability (Alkondon and Albuquerque, 1993; Castro and Albuquerque, 1995) and have been shown to regulate various forms of hippocampal synaptic plasticity (Kenney and Gould, 2008; Yakel, 2014). Depending on the location and timing, activation of α7 nAChRs can have different effects on hippocampal synaptic plasticity (Ge and Dani, 2005; Gu et al., 2012; Gu and Yakel, 2011; Ji et al., 2001). The α7 nAChRs are also highly expressed in hippocampal interneurons and thus can have complex effects on hippocampal pyramidal neuron activity due to inhibition and disinhibition (Ji and Dani, 2000). In addition, hippocampal interneurons have also been shown to regulate theta generation (Csicsvari et al., 1999; Dragoi et al., 1999). The α7 nAChRs therefore have the potential to influence theta by modulating hippocampal interneuron activities. The role of nAChRs and the potential neuronal populations involved in theta generation and strength have yet to be examined, however.

In this study, we infused the selective α7 nAChR antagonist methyllycaconitine (MLA) into the hippocampus *in vivo* and found that inhibition of hippocampal α7 nAChRs decreases theta power in running mice. Moreover, by selective KO of α7 nAChR in several neuronal subpopulations, we found that α7 nAChRs expressed on interneurons, particularly in OLM interneurons, contributed to type-I hippocampal theta generation.

## RESULTS

### Hippocampal α7 nAChRs Regulate Theta Power in Freely Moving Mice

We have previously found that mAChRs regulated hippocampal theta power in freely moving mice by infusion of the receptor antagonist atropine directly to the hippocampus (Gu et al., 2017). Here we infused nicotinic receptor antagonists to the hippocampus to examine whether they similarly regulate theta oscillations. Four randomized treatments were administrated to each mouse, including saline as a control, a selective α7 nAChR antagonist MLA, a selective α4-nAChR antagonist dihydro-β-erythroidine (DHβE), and a combination of MLA, DHβE, and atropine. The treatments were separated by at least three days to allow the mice to recover from the drug administrations. Theta oscillations were recorded through stainless steel wires that were attached around the unilateral infusion cannula targeting dorsal hippocampal CA1 *stratum lacunosum moleculare* (Figure S1A) where large-amplitude theta oscillations can be detected (Bragin et al., 1995). As expected, theta oscillations occurred mostly during running and active exploring, but not during immobile times, as shown in Figure 1A. The theta power was compared between saline and antagonist treatments only during running periods that lasted at least 10 s. Hippocampal infusion of MLA, but not DHβE, significantly reduced peak theta power during running (Figures 1A–1D), similar to our previously reported effect of hippocampal atropine infusion (Gu et al., 2017). A combination of MLA, DHβE, and atropine did not result in a significant further reduction of theta power than MLA alone. None of these antagonist treatments significantly changed the frequency of peak theta oscillations (Figure 1E). The open-field locomotor activity including velocity, total distance traveled, and immobility was not significantly changed among the various treatments (Figures S1B–S1D). In addition, receptor antagonist infusion had no significant effects on gamma oscillation peak power or peak frequency (Figures S1E and S1F).

Theta oscillations are strongly suggested to support spatial learning and memory (Buzsáki, 2005; Buzsáki and Moser, 2013; Givens and Olton, 1990; Hasselmo, 2005; Winson, 1978), and we have previously shown that the theta oscillations are closely related to Y-maze spontaneous alternation performance (Gu et al., 2017), which depends on spatial working memory (Hughes, 2004) and involves multiple brain regions including the hippocampus (Blampied and Wilby, 1975; Dillon et al., 2008; Lalonde, 2002; Means et al., 1971). Therefore, we tested whether nAChRs similarly regulated performance on this spatial memory task. Indeed, we found that hippocampal MLA infusion, but not DHβE, also impaired Y-maze spontaneous alternation performance (Figure 1F). A combination of MLA, DHβE, and atropine resulted in a slightly further (but not significant) impairment in Y-maze performance than MLA alone (Figure 1F). None of these antagonist treatments significantly changed the total numbers of Y-maze-arm entries (Figure 1G).

### α7 nAChR Activation Facilitates Future Theta Generation *In Vitro*

To understand the individual contributions of α7 nAChRs and mAChRs in theta generation, we turned to our *in vitro* septo-entorhinal-hippocampal brain slice tri-culture preparation (Gu and Yakel, 2017). To include the entorhinal cortex, the ventral hippocampus, which is connected to the entorhinal cortex, was used (Gu and Yakel, 2017). Theta-like oscillations, with a frequency of approximately 8–9 Hz, could be induced by pairing optical stimulation of septal cholinergic axons (10 pulses at 10 Hz) with hippocampal Schaffer collateral (SC) stimulation (one pulse within 100 ms after the last pulse of cholinergic stimulation). The field potential was recorded from the *stratum lacunosum moleculare* (slm) in area CA1 (Figure S2). Neither cholinergic nor SC stimulation alone could induce such oscillations (Figure 2A). Moreover, after 5–10 times of such pairings, the SC stimulation alone could induce theta-like oscillations. These results suggest that cholinergic pairing not only induces transient theta-like oscillations, but repeated pairing also primes the network to future theta generation by subsequent stimulation. Consistent with our *in vivo* results, bath application of the α7 nAChR antagonist MLA blocked the generation of theta-like oscillations in slice co-cultures, while α4β2 nAChR antagonist DHβE had no significant effects on

Please cite this article in press as: Gu et al., Hippocampal Interneuronal α7 nAChRs Modulate Theta Oscillations in Freely Moving Mice, Cell Reports (2020), https://doi.org/10.1016/j.celrep.2020.107740



CellPress
OPEN ACCESS

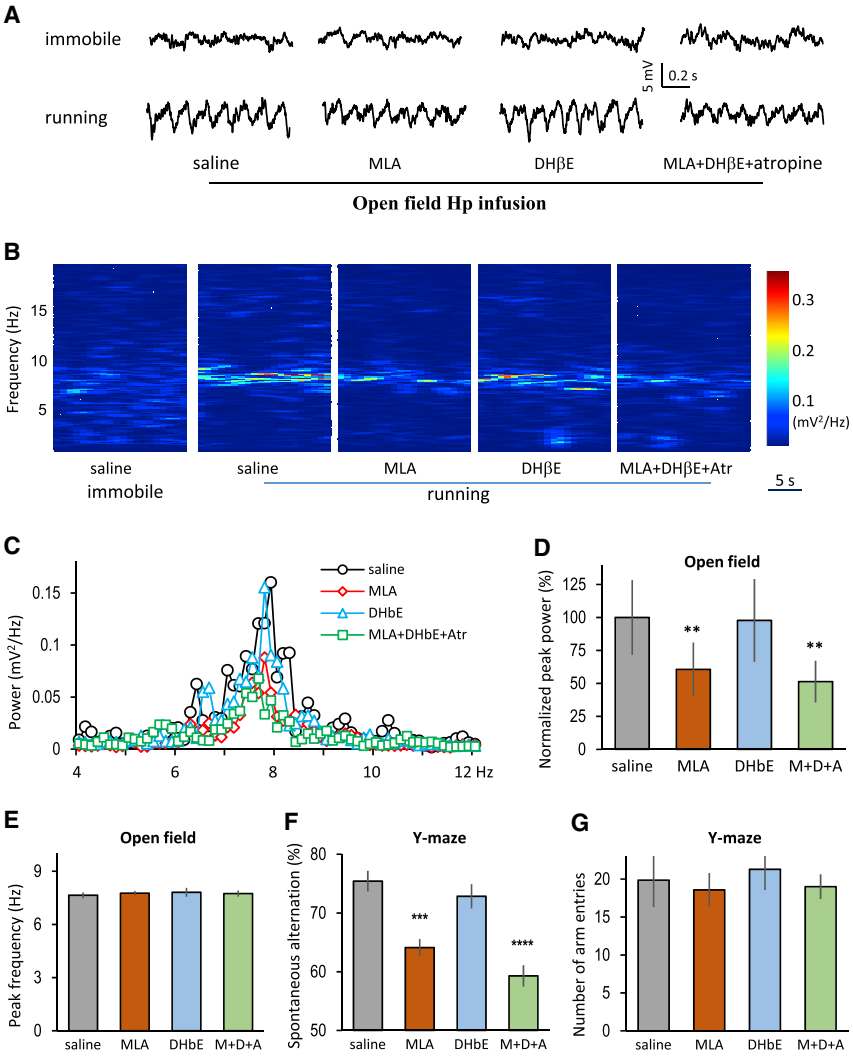


**Figure 1. Hippocampal α7 nAChRs Regulate Theta Power in Freely Moving Mice**

(A) Representative hippocampal local-field-potential recordings from one mouse freely moving in an open-field arena over four trials under various intrahippocampal cholinergic-receptor-antagonist infusion treatments.

(B) Spectrogram analysis of representative *in vivo* hippocampal-field-potential recordings (20 s) showing strong theta power during running. Theta power was reduced by hippocampal infusion of selective α7 nAChR-antagonist MLA, but not by selective α4β2-nAChR-antagonist DHβE. A combination of MLA with muscarinic-receptor-antagonist atropine did not result in significant further reduction of theta power.

(C) Power spectral density (PSD) analysis of representative recordings showing the power profile after various treatments.

(D) Bar graph showing normalized peak theta power after infusion of different receptor antagonists to ipsilateral hippocampus. p = 0.0098 (MLA), 0.9944 (DHβE), and 0.0019 (M+D+A [MLA + DHβE + Atropine]) compared with saline treatment, n = 6 mice per treatment group, one-way ANOVA, Dunnett post hoc test. The M+D+A treatment was not significantly different from MLA alone (p = 0.7589, n = 6 mice per treatment group, RM (repeated measures) one-way ANOVA, Dunnett post hoc test).

(E) Bar graph showing that peak theta frequency was not significantly changed by any antagonist treatments. p = 0.9325 between groups, n = 6 mice per group, RM one-way ANOVA.

(F) Bar graph showing that Y-maze spontaneous alternation task performance was impaired by hippocampal infusion of either MLA or a combination of M+D+A, but not by DHβE alone. p = 0.0005 for MLA, 0.5897 for DHβE, and < 0.0001 for M+D+A, compared with saline treatment, n = 7 mice per treatment group, RM one-way ANOVA, Dunnett post hoc test. The M+D+A treatment was not significantly different from MLA alone (p = 0.1473, n = 7 mice per treatment group, RM one-way ANOVA, Dunnett post hoc test).

(G) Bar graph showing that the total number of Y-maze arm entries was not significantly changed over the four treatments. p = 0.9157 between treatment groups, n = 7 mice per group, RM one-way ANOVA.

Data are represented as mean ± SEM.

either peak theta power or frequency (Figures 2B and 2C). In addition, neither MLA nor DHβE could block theta oscillations after induction (Figures 2D–2F).

Compared with mAChRs, α7 nAChRs are activated at higher ACh concentrations (Alkondon and Albuquerque, 1993; Kellar et al., 1985). To understand their individual contributions to theta generation, we paired high or low concentrations of ACh with SC stimulation in slice co-cultures *in vitro* (Figure 3). Similar theta-like oscillations were induced by pairing 1 s of 1 mM Ach, puff-applied by pico-spritzer to the hippocampus with SC stimulation (immediately after the ACh puff). After five pairings, SC stimulation alone could also induce theta-like oscillations (Figure 3A). In contrast, pairing 20 μM ACh with SC stimulation only induced theta-like oscillations during, but not after, the pairing (Figure 3B). Adding 0.1 mM choline (a selective α7 nAChR agonist) with 20 μM ACh enabled SC stimulation to induce theta-like oscillations after five pairings (Figure 3C). However, choline may also have an α7 nAChR-independent effect on hippocampal pyramidal neuron excitability and synaptic transmission (Albiñana et al., 2017). Whether this α7 nAChR-independent effect of choline contributed to theta-like oscillation is yet to be examined. The peak power and frequency of the theta-like oscillations induced were not significantly different between different concentrations of ACh or choline pairing (Figures 3E and 3F). The induction of theta-like oscillations by 20 μM ACh was blocked by atropine (Figures 3D and 3E). The theta-like oscillations usually last for about nine cycles (1 s) in most slices (Figure S3). These results suggest that mAChR activation at low ACh release may promote transient theta oscillations, while additional α7 nAChR activation at high ACh release may modify the network to facilitate future theta generation by subsequent stimulation.

Please cite this article in press as: Gu et al., Hippocampal Interneuronal α7 nAChRs Modulate Theta Oscillations in Freely Moving Mice, Cell Reports (2020), https://doi.org/10.1016/j.celrep.2020.107740



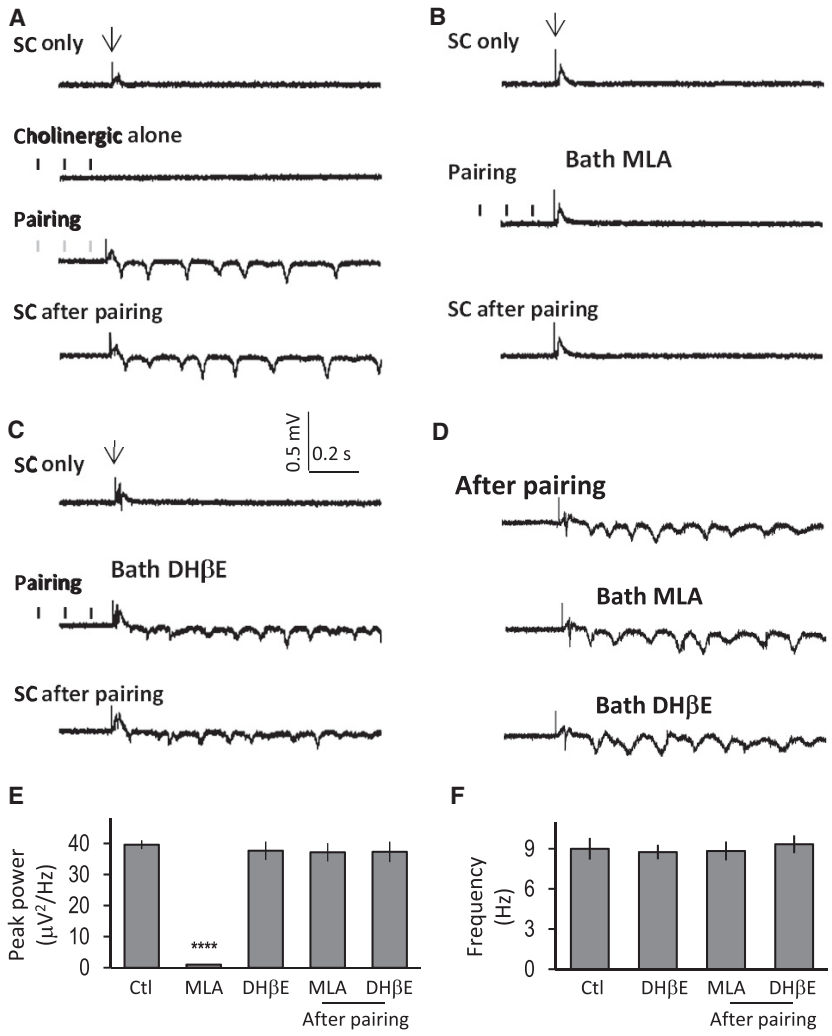


**Figure 2. α7 nAChRs Regulate the Induction of Theta-like Oscillations in Septo-entorhinal-Hippocampal Slice Co-cultures *In Vitro***

(A) Theta-like oscillations can be induced in septo-entorhinal-hippocampal slice co-cultures by pairing Schaffer collateral (SC) and cholinergic activation, but not by either pathway activation alone. After 5–10 pairings, SC stimulation alone could then induce theta-like oscillations.

(B and C) Representative traces showing that the induction of theta-like oscillations can be blocked by bath-applied MLA (B) but not by DHβE (C).

(D) Representative traces showing that the expression of theta-like oscillations after induction was not blocked by bath-applied MLA or DHβE.

(E and F) Bar graph of the peak power (E) and frequency (F) showing that the induction of theta-like oscillations was blocked by MLA ($p < 0.0001$) but not by DHβE ($p = 0.2798$), compared with control group. DHβE also did not change the frequency ($p = 0.8717$). n = 6 slices per group, t test.

Data are represented as mean ± SEM.

## α7 nAChRs Expressed in OLM Interneurons Regulate Theta Power

We have previously found that M1 mAChRs expressed on pyramidal neurons (but not interneurons) regulate theta oscillations (Gu et al., 2017), but the α7 nAChR activities have been observed from both hippocampal pyramidal neurons and interneurons (Ji et al., 2001). To identify the neuronal subpopulations that are involved in α7 nAChR-dependent theta generation, we first selectively knocked out α7 nAChRs in either pyramidal neurons or inhibitory interneurons by crossing Cre-dependent α7 nAChR conditional KO mice (Hernandez et al., 2014) with either CaMK2a-Cre or Gad2-Cre mice in which Cre is selectively expressed in either pyramidal neurons or interneurons, respectively. Unlike the case with the mAChRs (Gu et al., 2017), knocking out α7 nAChRs in interneurons significantly reduced peak theta power during active exploration in freely-moving mice, as compared to Cre-negative-floxed α7 nAChR control mice (Figures 4A–4C). Knocking out α7 nAChRs in pyramidal neurons resulted in a slight (but not significant) reduction of peak theta power. We further examined two interneuron subpopulations that were potentially involved in α7 nAChR-dependent theta generation, namely somatostatin (Sst)-positive and α2-nAChR-positive OLM (OLMα2) interneurons (Leão et al., 2012; Mikulovic et al., 2015; Siwani et al., 2018). Both reside mainly in the *stratum oriens* layer that receives rich septal cholinergic innervation (Gu and Yakel, 2011). OLMα2 interneurons are a subpopulation of Sst neurons and are selectively identified with α2-nAChR expression (Leão et al., 2012; Mikulovic et al., 2015; Siwani et al., 2018). However, these two groups of interneurons have also been shown to have opposite effects on SC to CA1 excitatory synaptic transmission (Leão et al., 2012; Lovett-Barron et al., 2012). We found that peak theta power during active exploration was significantly reduced in mice with α7 nAChR knocked out in OLMα2 interneurons, but not in mice with α7 nAChR knocked out in Sst interneurons (Figures 4A–4C). We found no significant change in peak frequency among mice with α7 nAChR knocked out in the different neuronal subpopulations we tested (Figure 4D). Y-maze spontaneous alternation performance was also impaired in mice with α7 nAChR globally knocked out in interneurons (i.e., GAD2) or in OLMα2 interneurons, but not in mice with α7 nAChR knocked out in pyramidal neurons or Sst interneurons (Figure 4E). The number of total Y-maze arm entries was not significantly changed among mice with α7 nAChR knocked out in different neuronal subpopulations (Figure 4F). The open-field locomotor activity including velocity, total distance traveled, and immobility was not significantly changed among different groups (Figures 4G–4I).

The potential cellular mechanisms underlying the contribution of α7 nAChR activation on OLMα2 neurons to theta generation were further explored in slice co-culture preparation *in vitro*.

Please cite this article in press as: Gu et al., Hippocampal Interneuronal α7 nAChRs Modulate Theta Oscillations in Freely Moving Mice, Cell Reports (2020), https://doi.org/10.1016/j.celrep.2020.107740



CellPress
OPEN ACCESS

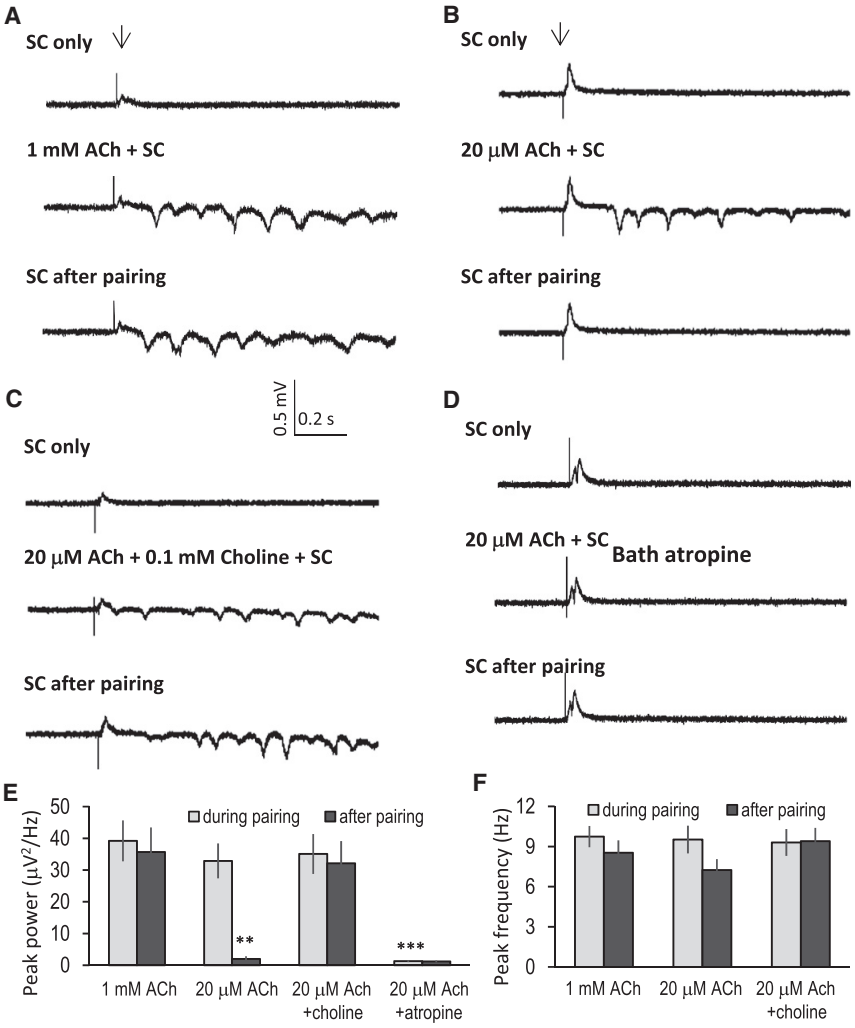


**Figure 3. α7 nAChR Activation Contributes to the Cholinergic-Pairing-Induced Plasticity**

(A) Pairing 1 mM ACh with SC stimulation induced theta-like oscillations in slice co-cultures. After five pairings, SC stimulation alone could induce similar oscillations.

(B) Pairing 20 μM ACh with SC stimulation also induced theta-like oscillations in slice co-cultures. However, after five pairings, SC stimulation alone could not induce oscillations.

(C) Pairing 20 μM ACh plus 0.1 mM choline with SC stimulation induced theta-like oscillations. After five pairings, SC stimulation alone could induce similar oscillations.

(D) The induction of theta-like oscillations by pairing 20 μM ACh with SC stimulation was blocked by bath-applied atropine.

(E) Bar graph of the peak powers showing that theta-like oscillations could be induced by pairing SC stimulation with either 1 mM ACh or 20 μM ACh, or 20 μM ACh plus 0.1 mM choline. However, SC stimulation alone could induce theta-like oscillations only after repeated pairing with either 1 mM ACh or 20 μM ACh plus 0.1 mM choline, but not after pairing with 20 μM ACh only. **p = 0.0045, ***p = 0.0004 compared with 20 μM ACh during pairing. n = 5 slices for each group, t test.

(F) The frequency of the oscillations did not change significantly among different treatments. p = 0.4359. n = 5 slices for each group, one-way ANOVA.

Data are represented as mean ± SEM.

We have previously shown that cholinergic pairing that induced theta-like oscillations also enabled induction of LTP (long-term potentiation) of SC to CA1 pyramidal excitatory synaptic currents (EPSCs; Gu et al., 2017). Cholinergic inputs were activated via ChR2 by 10 pulses of 20 ms of laser light (488 nm at 10 mW) at 10 Hz, 1 s before SC stimulation. Here we find that this LTP was blocked by the selective α7 nAChR antagonist MLA (Figure 5A), suggesting a requirement for α7 nAChR activation. Further, the LTP was also significantly impaired in slices from mice with α7 nAChR knocked out in OLMα2 interneurons (Figure 5B), again specifically implicating the OLMα2 interneurons. Indeed, excitatory synaptic responses from OLMα2 interneurons induced by SC stimulation were also enhanced in control OLMα2-Cre mice, but not in OLMα2-α7 nAChR KO mice (Figures 5C and 5D). These results suggest that cholinergic pairing increased OLMα2-interneuron activity through α7 nAChR activation, which may have in turn enhanced CA1 pyramidal responses to SC stimulation. This was further confirmed in our slice co-culture preparation that showed increased amplitude of SC to CA1 pyramidal EPSCs by direct OLMα2-interneuron activation via ChR2 (Figures 5E and 5F), likely through di-synaptic disinhibition by inhibiting *stratum* radiatum interneurons that provide feed-forward inhibition onto pyramidal neurons after SC excitation (Figures 5G–5I), as suggested by a previous study (Leão et al., 2012). Moreover, we found that repeated pairing of OLMα2-interneuron activation and SC stimulation induced enhanced EPSCs from pyramidal neurons not only during the pairing, but also after the pairing. Repeated pairing of Sst interneuron activation and SC stimulation reduced EPSCs from pyramidal neurons during the pairing but had no effect after the pairing (Figures 5E and 5F). Repeated pairing of OLMα2-interneuron activation and SC stimulation also transiently reduced inhibitory postsynaptic current (IPSC) responses from CA1 pyramidal neurons, while repeated pairing of Sst interneuron activation and SC stimulation transiently increased IPSCs (Figures 5G and 5H), suggesting the presence of disinhibition after OLMα2-interneuron activation in the cultured slices.

We then verified the effectiveness of selective α7 nAChR KO in Cre-expressing neuronal subpopulations. Cre-positive neurons were visualized by viral expression of Cre-dependent fluorescent protein mCherry in cultured slices (Figure 6A). OLMα2-Cre-positive neurons were mainly located in the CA1 *stratum oriens* with extensive axonal projections to the slm, similar to the pattern shown in the previous study (Leão et al., 2012). Sst-Cre-positive neurons were distributed beyond CA1, e.g., in CA3 and DG. Gad2-Cre-positive neurons were distributed throughout the

Please cite this article in press as: Gu et al., Hippocampal Interneuronal α7 nAChRs Modulate Theta Oscillations in Freely Moving Mice, Cell Reports (2020), https://doi.org/10.1016/j.celrep.2020.107740



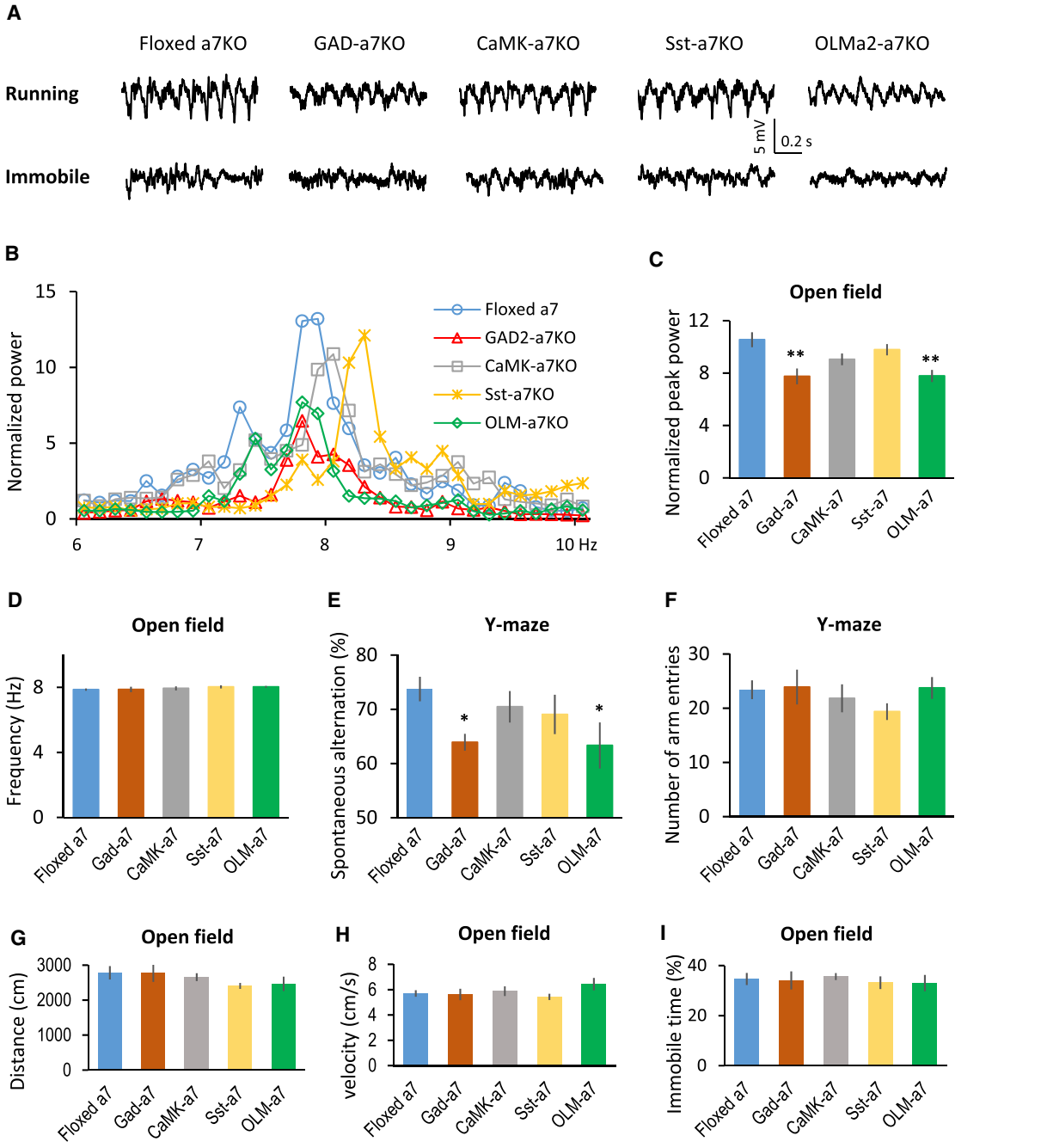


**Figure 4. α7 nAChRs Expressed in OLMα2 Interneurons Regulate Theta Power and Y-Maze Spontaneous Alternation Performance**

(A) Representative hippocampal local field potential recordings from mice with α7 nAChR knocked out in interneurons (GAD-α7KO, GAD2-Cre/floxed α7 nAChR), pyramidal neurons (CaM2a-α7KO, CaMK2a-Cre/floxed α7 nAChR), Sst-positive interneurons (Sst-α7KO, Sst-Cre/floxed α7 nAChR), OLMα2-positive interneurons (OLMα2-α7KO, OLMα2-Cre/floxed α7 nAChR), or $Cre^{-}$/floxed α7 nAChR control mice (floxed α7KO).

(B) PSD analysis of representative recordings from mice with α7 nAChR KO in different neuronal subpopulations.

(C) Bar graph showing reduced peak theta power from mice with α7 nAChR KO in interneurons ($p = 0.0047$), OLMα2-positive interneurons ($p = 0.0083$), but not in pyramidal neurons ($p = 0.2354$) or Sst-positive interneurons ($p = 0.8047$), as compared with floxed controls, n = 8 mice per group except for floxed controls (n = 20), one-way ANOVA, Dunnett post hoc test.

(D) Bar graph showing that theta frequency was not significantly changed among the α7 nAChR KO groups. $p = 0.6620$ between groups, n = 8 mice per group except for floxed controls (n = 20), one-way ANOVA.

*(legend continued on next page)*

Please cite this article in press as: Gu et al., Hippocampal Interneuronal α7 nAChRs Modulate Theta Oscillations in Freely Moving Mice, Cell Reports (2020), https://doi.org/10.1016/j.celrep.2020.107740





subregions and strata of the hippocampus. CaMKII-Cre-positive neurons were mainly distributed in the *stratum pyramidale*. All these Cre expression patterns are consistent with *in vivo* expression patterns shown in previous studies (Leão et al., 2012; Luikart et al., 2005; Taniguchi et al., 2011; Tsien et al., 1996). We recorded choline-induced α7 nAChR currents in these Cre-positive neurons and found that the current amplitude is larger in interneurons than pyramidal neurons, consistent with previous observations (Yakel, 2014). Furthermore, OLMα2 cells had the largest α7 nAChR current among all the groups. All of the currents in the Cre-positive cells were absent in Cre/floxed α7 nAChR mice, showing the effective KO of the α7 nAChR receptors in Cre-positive cells (Figures 6B and 6C).

We also examined α7 nAChR expression *in vivo* by *in situ* hybridization. α7 nAChRs are expressed in GAD2, Sst, and CaMKII-positive neurons in the hippocampus, and the expression was effectively knocked out in these neurons from Cre/floxed α7 nAChR mice (Figures S4 and S5). However, α7 nAChRs are also expressed outside of the hippocampus (Séguéla et al., 1993), including the medial septum (Figures S6 and S7), and are effectively knocked out in these neurons from Cre/floxed α7 nAChR mice. The genetic targeting of α7 nAChRs will thus likely impact not only the neuronal subpopulations in the hippocampus, but also in other brain subregions outside of the hippocampus. The medial septum is known to be critical for hippocampal theta generation, although the cellular mechanisms are not clear. The α7 nAChRs expressed in the medial septum thus may regulate septal network activities and in turn regulate hippocampal theta generation. However, this is less of a concern than knocking out α7 nAChRs in α2-Cre-positive neurons since there is little α7 nAChR expression in α2-Cre-positive (tdTomato-positive) neurons in the medial septum in α2-Cre/Rosa tdTomato mice (0.9% out of 325 tdTomato-positive neurons from nine septal slices from three mice; Figure S8). Meanwhile, α7 nAChRs are indeed expressed in more than half of α2-tdTomato-positive neurons in hippocampal CA1 area in α2-Cre/Rosa tdTomato mice (56% out of a total of 124 tdTomato-positive cells from 15 hippocampal slices from three mice; Figure 7C) and the expression was effectively eliminated in α2-Cre/Rosa tdTomato/floxed α7 nAChR mice (only one α2-*in-situ*-staining-positive cell out of 111 tdTomato-positive cells from 15 hippocampal slices of three mice; Figure 7D). These hippocampal α2-Cre-positive neurons have the typical features of OLM neurons, with cell bodies in SO (stratum oriens) of CA1 and extensive axonal projections in SLM of CA1 (Figure 7A). These α2-Cre-positive neurons were further verified by chrna2 *in situ* hybridization that they were indeed α2-expressing neurons (Figures 7B and S8A); 91% of α2-tdTomato-positive cells (109 cells from 15 hippocampal slices from three mice) are chrna2 positive, while 97% of chrna2 *in-situ*-positive cells (102 cells from 15 hippocampal slices from three mice) are also α2-tdTomato positive in the hippocampal CA1 area. Similar results were observed in the medial septum, with 92% of α2-tdTomato-positive cells (343 cells) were chrna2-*in-situ* positive, while 96% of chrna2-*in-situ*-positive cells (326 cells) were also α2-tdTomato positive in the medial septal area (nine septal slices from three mice).

## DISCUSSION

The results presented here provide evidence that in addition to mAChRs, hippocampal α7 nAChRs also regulate hippocampal theta oscillations. Although M1 mAChRs are mainly expressed in CA1 pyramidal neurons in the hippocampus (Levey et al., 1995), and our previous study suggested that M1 mAChRs mainly targeted pyramidal neurons in the CA1 hippocampal region to promote theta generation (Gu et al., 2017), the current study suggests that α7 nAChRs mainly targeted interneurons, particularly the OLMα2 interneurons, in promoting theta generation. However, rather than as an independent mechanism, hippocampal α7 nAChRs likely work together with mAChRs in promoting theta oscillations, because inhibition of both receptors did not produce significant further theta impairment than inhibition of either of the receptors alone. Through the activation of different subtypes of cholinergic receptors in different neuronal subpopulations, acetylcholine likely modulates different aspects of theta oscillations to support a variety of behaviors and functions. Hippocampal theta oscillations are strongly implicated in supporting spatial learning and memory (Buzsáki, 2005; Buzsáki and Moser, 2013; Givens and Olton, 1990; Hasselmo, 2005; Winson, 1978). Indeed, treatments including hippocampal infusion of an α7 nAChR antagonist or knocking out α7 nAChRs in OLMα2 interneurons, that reduced theta power in open-field exploration, also impaired memory performance in a Y-Maze spontaneous alternation task that heavily relies on spatial working memory (Hughes, 2004) and involves multiple brain regions including the septo-hippocampal system (Lalonde, 2002). Our study further suggests that theta oscillations may underlie the septo-hippocampal involvement. These observations thus strongly suggest an important role for α7 nAChRs in regulating hippocampal theta oscillations and subsequent behavioral performance.

The mAChRs can be activated with relatively low concentrations of ACh, which usually leads to increased excitation of target cells (Kellar et al., 1985). In contrast, the α7 nAChRs are activated with higher ACh concentrations and leads to calcium influx into target cells (Alkondon and Albuquerque, 1993; Castro and Albuquerque, 1995). In a general sense, these two receptors may work in a similar fashion as the AMPA/NMDA glutamate

(E) Bar graph showing that Y-maze spontaneous alternation task performance was impaired in mice with the α7 nAChR KO in interneurons ($p = 0.0119$) and OLMα2 interneurons ($p = 0.0239$), but not in pyramidal neurons ($p = 0.4085$) or Sst interneurons ($p = 0.3177$), as compared with floxed controls, $n = 10$ mice per group except for floxed controls ($n = 25$), one-way ANOVA, Dunnett post hoc test.

(F) Bar graph showing that the total number of Y-maze arm entries was not significantly changed among the groups ($p = 0.7546$, $n = 10$ mice per group except for floxed controls (25), one-way ANOVA).

(G–I) Open-field locomotor activity including total distance traveled (G, $p = 0.61$), velocity (H, $p = 0.46$), and immobility (I, $p = 0.98$) was not significantly changed among various groups. $n = 8$ mice per group except for floxed controls ($n = 20$), one-way ANOVA.

Data are represented as mean ± SEM.

Please cite this article in press as: Gu et al., Hippocampal Interneuronal α7 nAChRs Modulate Theta Oscillations in Freely Moving Mice, Cell Reports (2020), https://doi.org/10.1016/j.celrep.2020.107740



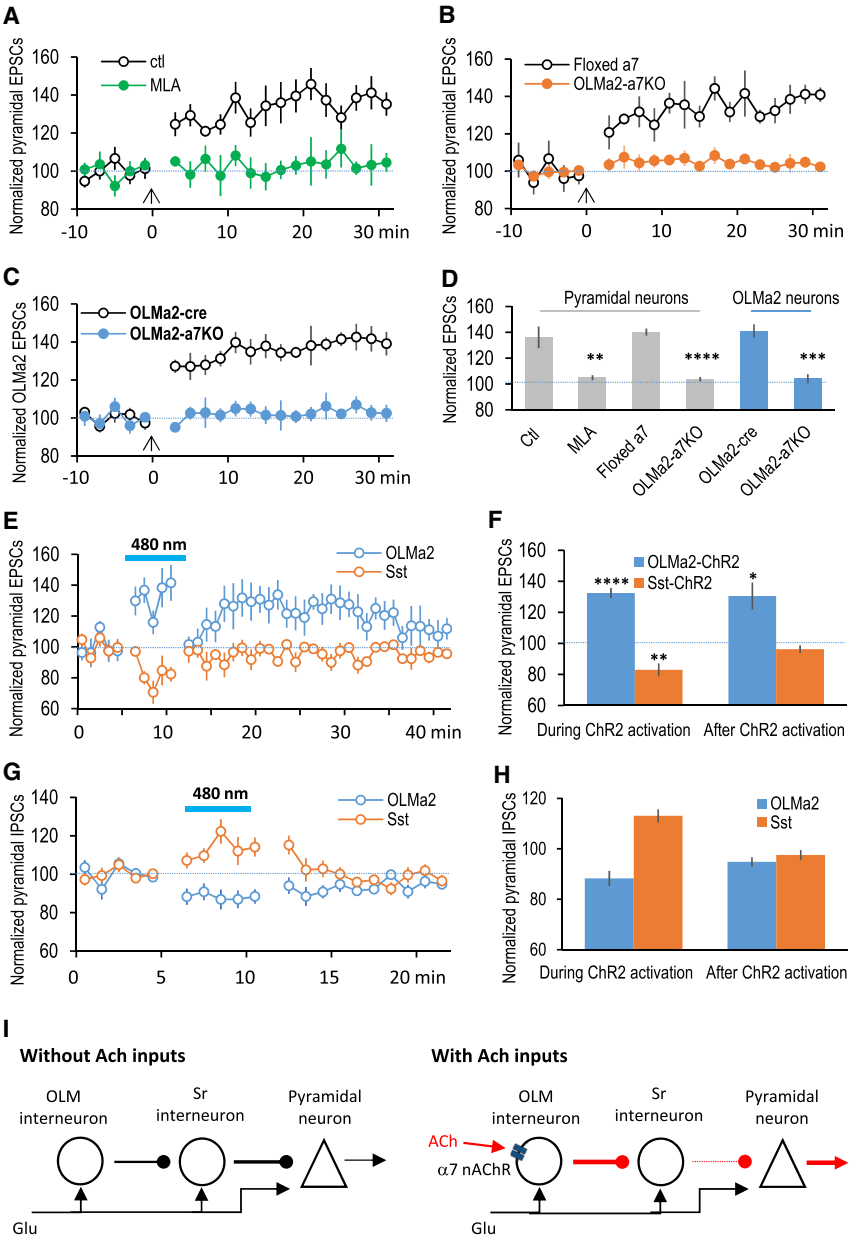


**Figure 5. α7 nAChRs on OLMα2 Interneurons Are Involved in Cholinergic Pairing-Induced Hippocampal Synaptic Plasticity**

(A) Normalized SC-evoked EPSC responses from CA1 pyramidal neurons showing that the enhancement of hippocampal excitatory transmission by cholinergic pairing (at the time of 0 min as indicated by the arrow) can be blocked by bath applied selective α7 nAChR antagonist MLA.

(B) Normalized SC-evoked EPSC responses from CA1 pyramidal neurons showing that the enhancement of EPSCs was impaired in hippocampal slices from mice with selective α7 nAChR KO in OLMα2 interneurons.

(C) Normalized SC-evoked EPSC responses from OLMα2 interneurons showing that EPSCs of OLMα2 interneurons were also enhanced by cholinergic pairing and the enhancement was impaired in hippocampal slices from mice with selective α7 nAChR KO in OLMα2 interneurons.

(D) Bar graph showing that cholinergic-pairing-induced LTP of SC-evoked pyramidal EPSCs was blocked by MLA ($p = 0.0047$, compared with control slices, $n = 6$ slices for each group, t test) and impaired in slices from mice with selective α7 nAChR KO in OLMα2 interneurons ($p < 0.0001$, compared with floxed control mice, $n = 5$ slices for each group, t test). The cholinergic-pairing-induced LTP of SC-evoked OLMα2 EPSCs was also impaired in slices from OLMα2-α7 nAChR KO mice ($p = 0.0004$, compared with floxed control mice, $n = 5$ slices for each group, t test).

(E) Normalized SC-evoked EPSC responses from CA1 pyramidal neurons showing increased EPSC amplitude when SC stimulation was paired with OLMα2- interneuron activation (via ChR2, 1 s of 10-mW, 488-nm laser light delivered 1 s before SC stimulation). After five times of pairing, the EPSC enhancement lasted at least for 10 min after the pairing. On the contrary, the EPSC amplitude was reduced when SC stimulation was paired with Sst interneuron activation. The EPSC amplitude returned to baseline immediately after five pairings.

(F) Bar graph showing that SC-evoked pyramidal EPSC amplitude was increased by pairing with OLMα2-interneuron activation ($p < 0.0001$ during pairing, $p = 0.015$ at 10 min after pairing, compared with baseline before pairing, $n = 5$ slices for each group, t test). On the other hand, EPSC amplitude was decreased by pairing with Sst interneuron activation but returned to baseline immediately after the pairing ($p = 0.0041$ during pairing, $p = 0.1583$ at 10 min after pairing, compared with baseline before pairing. $n = 5$ slices for each group, t test).

(G) Normalized SC-evoked IPSC responses from CA1 pyramidal neurons showing decreased IPSC amplitude when SC stimulation was paired with OLMα2 interneuron activation. The IPSC amplitude was increased when SC stimulation was paired with Sst interneuron activation.

(H) Bar graph showing that SC-evoked-pyramidal IPSC amplitude was decreased by pairing with OLMα2-interneuron activation ($p = 0.031$ during pairing, $p = 0.20$ at 10 min after pairing, compared with baseline before pairing, $n = 5$ slices for each group, t test). On the other hand, IPSC amplitude was increased by pairing with Sst interneuron activation but returned to baseline immediately after the pairing ($p = 0.029$ during pairing, $p = 0.38$ at 10 min after pairing, compared with baseline before pairing. $n = 5$ slices for each group, t test).

(I) Schematic drawing showing that ACh release may increase OLM interneuron excitability through α7 nAChR activation, resulting in increased inhibition onto *stratum radiatum* (Sr) interneurons that target pyramidal cells at the same dendritic compartment as the SC inputs, thereby reducing inhibition from Sr interneurons to pyramidal neurons and increasing pyramidal excitatory responses to SC excitation.

Data are represented as mean ± SEM.

receptors on synaptic transmission; mAChR activation may transiently excite the target cells (although more slowly than the AMPA receptors), while α7 nAChR activation may facilitate the upregulation of excitability by playing a more prominent role in modifying synaptic plasticity in part through calcium influx (similar to the NMDA receptors). Our *in vitro* slice study suggests

Please cite this article in press as: Gu et al., Hippocampal Interneuronal α7 nAChRs Modulate Theta Oscillations in Freely Moving Mice, Cell Reports (2020), https://doi.org/10.1016/j.celrep.2020.107740



CellPress
OPEN ACCESS

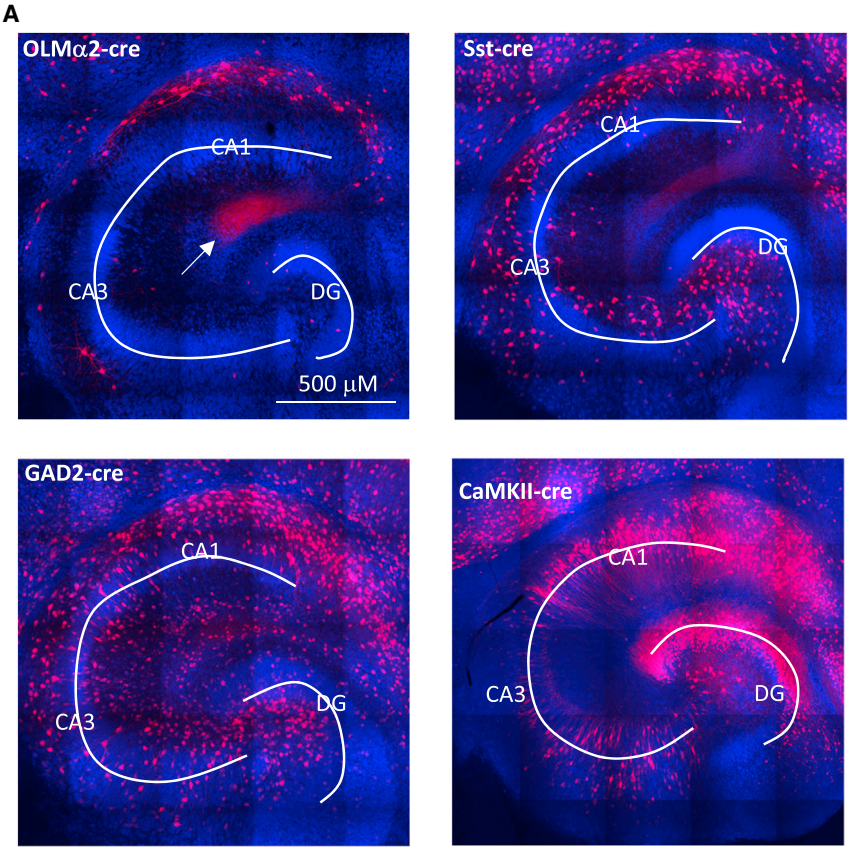


**Figure 6. α7 nAChR-Mediated Currents Were Effectively Knocked Out in Cre-Positive Neurons from Cre/Floxed α7 nAChR Mice**

(A) Images showing the distribution of Cre-positive neurons in the hippocampus in the cultured slices. Cre-positive neurons were visualized with Cre-dependent mCherry expression (red color). The slices were counterstained with DAPI (blue). OLMα2-positive neurons were primarily located in CA1 *stratum oriens*. Sst-positive neurons had a much broader distribution than OLMα2 neurons. GAD2 neurons were widely distributed throughout hippocampal subregions and strata. CaMKII neurons were primarily distributed in *stratum pyramidale* and DG granular cell layer.

(B) Choline-induced α7 nAChR currents were detected in all of the four neuronal subpopulations examined. OLMα2 neurons showed the largest current among the four groups while CaMKII-positive neurons showed the smallest current. The current was absent in the Cre-positive neurons from Cre/floxed α7 nAChR mice. Red bars indicate the time choline (10 mM, 50 ms) was applied.

(C) Bar graph shows that α7 nAChR current was absent from Cre/floxed α7 nAChR mice. $p < 0.0001$ as compared with cells from Cre-only mice, $n = 8$ cells from at least three mice in each group, t test. Data are represented as mean ± SEM.

that mAChRs activated by low concentrations of ACh mainly promote transient theta oscillations, while activation of both mAChRs and α7 nAChRs with higher concentrations of ACh may prime the network to future theta induction by subsequent stimulation.

Theta oscillations have been closely related to memory encoding (Battaglia et al., 2011; Buzsáki, 2002, 2005; Buzsáki and Moser, 2013; Hasselmo, 2005; Winson, 1978). Previous studies have focused on the potential effects of theta oscillations on synaptic plasticity induction (Buzsáki, 2002; Igarashi, 2015). On the other hand, neurotransmitter receptors involved in theta generation, including both cholinergic receptors and NMDA receptors, are known to promote memory encoding through modulating synaptic plasticity. Cholinergic receptors and NMDA receptors thus may not only promote transient theta generation, but also may modify theta oscillations by stabilizing the neuronal population activity underlying theta oscillations through synaptic plasticity. The same neuronal populations and associated theta oscillations may be reactivated later by familiar stimuli. Indeed, theta frequency is lower in a novel environment and higher in a familiar environment (Jeewajee et al., 2008b; Wells et al., 2013), suggesting that theta oscillations are indeed modified by experience, and the modified features can be stably expressed afterward in the familiar environment.

Unlike AMPA/NMDA receptors that act on the same individual synapses, mAChR/α7 nAChR may coordinate at the network level by engaging different neuronal subpopulations. Although M1 AChRs contribute to theta generation mainly through regulating pyramidal neuronal activities, α7 nAChRs contribute to theta generation mainly through modulating interneuronal activation, particularly OLMα2-interneuronal activities. Interestingly, a recent study directly linked OLMα2 interneurons to theta oscillations (Mikulovic et al., 2018). Inhibition of OLMα2 interneurons reduced tail-pinch-induced type-II theta power in mice under anesthesia, and activation of these OLMα2 interneurons induced 3–8 Hz theta oscillations under anesthesia. In treadmill-running mice, activation of OLMα2 interneurons induced a 7-Hz oscillation in addition to the 8-Hz type-I theta through modulating

Please cite this article in press as: Gu et al., Hippocampal Interneuronal α7 nAChRs Modulate Theta Oscillations in Freely Moving Mice, Cell Reports (2020), https://doi.org/10.1016/j.celrep.2020.107740



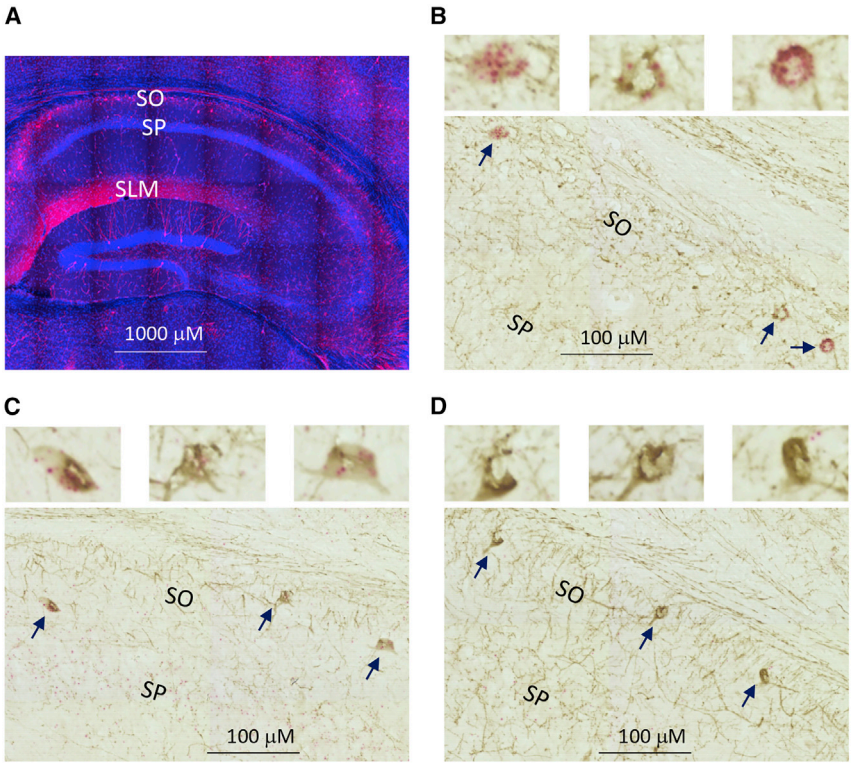


**Figure 7. *In Situ* Hybridization Showing α7 nAChRs Are Expressed in α2-Positive Neurons in the Hippocampus**

(A) Hippocampal α2-Cre-positive neurons have the typical features of OLM neurons. α2-Cre-positive neurons (visualized by tdTomato expression in α2-Cre/Rosa tdTomato mouse, red color) are mainly located in SO of CA1 with extensive axonal projection to SLM.

(B) Hippocampal α2-Cre-positive neurons (tdTomato positive, brown color, pointed by arrows, with enlarged images on top of the panel) show positive α2 expression (red color, *in situ* chrna2 staining).

(C) α7 nAChRs (red color, *in situ* chrna7 staining) are expressed in α2-Cre-positive neurons (tdTomato positive, brown color) in α2-Cre/Rosa tdTomato mouse.

(D) α7 nAChR expression (red color, *in situ* chrna7 staining) was effectively eliminated in α2-Cre-positive neurons (tdTomato positive, brown color) in α2-Cre//Rosa tdTomato/floxed α7 nAChR mouse.

pyramidal neuronal activities (Mikulovic et al., 2018). OLM interneurons were also among the neurons that had activity that was phase-locked to theta rhythm *in vivo* (Klausberger et al., 2003), and have been proposed as rhythm generators in computational models (Chatzikalymniou and Skinner, 2018; Gloveli et al., 2005; Hummos and Nair, 2017; Neymotin et al., 2013). One model suggested that OLM interneurons are only engaged by high cholinergic states in theta generation (Hummos and Nair, 2017), presumably involving α7 nAChRs that are activated with higher concentrations of acetylcholine.

Although OLMα2 interneurons are also Sst positive (Leão et al., 2012), the subpopulation of non-OLMα2-Sst neurons may have an opposite effect than OLMα2 neurons on SC to CA1 excitatory synaptic transmission. Previous studies showed that OLMα2 interneurons and Sst interneurons have opposite effects on SC to CA1 excitatory synaptic transmission (Leão et al., 2012; Lovett-Barron et al., 2012). Although inhibition of Sst neurons increases pyramidal cell responses to SC stimulation through dendritic disinhibition (Lovett-Barron et al., 2012), activation of OLMα2 interneurons increases SC to CA1 transmission, likely also through disinhibition by inhibiting *stratum radiatum* interneurons that provide feed-forward inhibition onto pyramidal neurons after SC excitation (Leão et al., 2012). Moreover, OLMα2 interneurons express α7 nAChR current (Haam et al., 2018; Leão et al., 2012) and are likely involved in nicotine-facilitated SC to CA1 LTP (Leão et al., 2012). Consistent with these studies, we found that even though activation of Sst interneurons in hippocampal slices transiently reduced SC to CA1 EPSCs and increased iPSCs, activation of OLMα2 interneurons, in contrast, increased SC to CA1 EPSCs and reduced iPSCs. Pairing cholinergic activation with SC excitation induced LTP in both CA1 pyramidal neurons and OLMα2 interneurons in an α7 nAChR-dependent manner. These results suggest that α7 nAChR activation can increase OLMα2 activity that, in turn, can enhance CA1 pyramidal responses after SC excitation, which may have facilitated the *in vitro* theta generation in our slice preparation.

Hippocampal theta oscillations corelate with a variety of behaviors and functions (Korotkova et al., 2018), likely through engaging different neuronal populations and cellular mechanisms at different times. Our current study indicates that by engaging different cholinergic receptor subtypes and neuronal subpopulations under different conditions, cholinergic transmission can modulate different aspects of theta oscillations to support various functions.

## STAR★METHODS

Detailed methods are provided in the online version of this paper and include the following:

- KEY RESOURCES TABLE
- RESOURCE AVAILABILITY
  - Lead Contact
  - Materials Availability
  - Data and Code Availability
- EXPERIMENTAL MODEL AND SUBJECT DETAILS

## SUPPLEMENTAL INFORMATION

Supplemental Information can be found online at https://doi.org/10.1016/j.celrep.2020.107740.

## ACKNOWLEDGMENTS

We thank Dr. Jesse Cushman and Korey Stevanovic for assistance with animal behavior tests and *in vivo* recordings, Patricia Lamb for animal genotyping and plasmid preparation, Dr. Bernd Gloss for AAV virus packaging, and Dr. James M. Wilson at the University of Pennsylvania for providing the AAV serotype 9 helper plasmid. This research was supported by the Intramural Research Program of the NIH, National Institute of Environmental Health Sciences/NIH/DHHS. B.G. acknowledges support from the Russian Academic Excellence Project 5-100. I.G. and B.G. received partial support from Labex ANR-10-LABX-0087 IEC, IDEX ANR-10-IDEX-0001-02 PSL*, and Foundation Alzheimer.

## AUTHOR CONTRIBUTIONS

Z.G. and J.L.Y. conceived of the project; Z.G., K.G.S., and G.M.A. performed the experiments; Z.G., I.G., and B.G. analyzed the data; Z.G. and J.L.Y. prepared the manuscript; and P.J. and S.M.D. provided input on the manuscript.

## DECLARATION OF INTERESTS

The authors declare no competing interests.

Received: December 11, 2018
Revised: April 3, 2020
Accepted: May 14, 2020
Published: June 9, 2020

## REFERENCES

Albiñana, E., Luengo, J.G., Baraibar, A.M., Muñoz, M.D., Gandía, L., Solís, J.M., and Hernández-Guijo, J.M. (2017). Choline induces opposite changes in pyramidal neuron excitability and synaptic transmission through a nicotinic receptor-independent process in hippocampal slices. Pflugers Arch. *469*, 779–795.

Alkondon, M., and Albuquerque, E.X. (1993). Diversity of nicotinic acetylcholine receptors in rat hippocampal neurons. I. Pharmacological and functional evidence for distinct structural subtypes. J. Pharmacol. Exp. Ther. *265*, 1455–1473.

Battaglia, F.P., Benchenane, K., Sirota, A., Pennartz, C.M., and Wiener, S.I. (2011). The hippocampus: hub of brain network communication for memory. Trends Cogn. Sci. *15*, 310–318.

Blampied, N.M., and Wilby, C.M. (1975). Effects of 3-acetylpyridine on spontaneous alternation in the mouse. Pharmacol. Biochem. Behav. *3*, 317–319.

Bragin, A., Jandó, G., Nádasdy, Z., Hetke, J., Wise, K., and Buzsáki, G. (1995). Gamma (40–100 Hz) oscillation in the hippocampus of the behaving rat. J. Neurosci. *15*, 47–60.

Bush, D., Bisby, J.A., Bird, C.M., Gollwitzer, S., Rodionov, R., Diehl, B., McEvoy, A.W., Walker, M.C., and Burgess, N. (2017). Human hippocampal theta power indicates movement onset and distance travelled. Proc. Natl. Acad. Sci. USA *114*, 12297–12302.

Buzsáki, G. (2002). Theta oscillations in the hippocampus. Neuron *33*, 325–340.

Buzsáki, G. (2005). Theta rhythm of navigation: link between path integration and landmark navigation, episodic and semantic memory. Hippocampus *15*, 827–840.

Buzsáki, G., and Moser, E.I. (2013). Memory, navigation and theta rhythm in the hippocampal-entorhinal system. Nat. Neurosci. *16*, 130–138.

Castro, N.G., and Albuquerque, E.X. (1995). alpha-Bungarotoxin-sensitive hippocampal nicotinic receptor channel has a high calcium permeability. Biophys. J. *68*, 516–524.

Chatzikalymniou, A.P., and Skinner, F.K. (2018). Deciphering the contribution of oriens-lacunosum/moleculare (OLM) cells to intrinsic θ rhythms using biophysical local field potential (LFP) models. eNeuro *5*, ENEURO.0146-18.2018.

Csicsvari, J., Hirase, H., Czurkó, A., Mamiya, A., and Buzsáki, G. (1999). Oscillatory coupling of hippocampal pyramidal cells and interneurons in the behaving Rat. J. Neurosci. *19*, 274–287.

Dannenberg, H., Pabst, M., Braganza, O., Schoch, S., Niediek, J., Bayraktar, M., Mormann, F., and Beck, H. (2015). Synergy of direct and indirect cholinergic septo-hippocampal pathways coordinates firing in hippocampal networks. J. Neurosci. *35*, 8394–8410.

Dillon, G.M., Qu, X., Marcus, J.N., and Dodart, J.C. (2008). Excitotoxic lesions restricted to the dorsal CA1 field of the hippocampus impair spatial memory and extinction learning in C57BL/6 mice. Neurobiol. Learn. Mem. *90*, 426–433.

Dragoi, G., Carpi, D., Recce, M., Csicsvari, J., and Buzsáki, G. (1999). Interactions between hippocampus and medial septum during sharp waves and theta oscillation in the behaving rat. J. Neurosci. *19*, 6191–6199.

Ge, S., and Dani, J.A. (2005). Nicotinic acetylcholine receptors at glutamate synapses facilitate long-term depression or potentiation. J. Neurosci. *25*, 6084–6091.

Givens, B.S., and Olton, D.S. (1990). Cholinergic and GABAergic modulation of medial septal area: effect on working memory. Behav. Neurosci. *104*, 849–855.

Gloveli, T., Dugladze, T., Rotstein, H.G., Traub, R.D., Monyer, H., Heinemann, U., Whittington, M.A., and Kopell, N.J. (2005). Orthogonal arrangement of rhythm-generating microcircuits in the hippocampus. Proc. Natl. Acad. Sci. USA *102*, 13295–13300.

Gogolák, G., Stumpf, C., Petsche, H., and Sterc, J. (1968). The firing pattern of septal neurons and the form of the hippocampal theta wave. Brain Res. *7*, 201–207.

Goutagny, R., Jackson, J., and Williams, S. (2009). Self-generated theta oscillations in the hippocampus. Nat. Neurosci. *12*, 1491–1493.

Green, J.D., and Arduini, A.A. (1954). Hippocampal electrical activity in arousal. J. Neurophysiol. *17*, 533–557.

Gu, Z., and Yakel, J.L. (2011). Timing-dependent septal cholinergic induction of dynamic hippocampal synaptic plasticity. Neuron *71*, 155–165.

Gu, Z., and Yakel, J.L. (2017). Inducing theta oscillations in the entorhinal hippocampal network in vitro. Brain Struct. Funct. *222*, 943–955.

Gu, Z., Lamb, P.W., and Yakel, J.L. (2012). Cholinergic coordination of presynaptic and postsynaptic activity induces timing-dependent hippocampal synaptic plasticity. J. Neurosci. *32*, 12337–12348.

Gu, Z., Alexander, G.M., Dudek, S.M., and Yakel, J.L. (2017). Hippocampus and entorhinal cortex recruit cholinergic and NMDA receptors separately to generate hippocampal theta oscillations. Cell Rep. *21*, 3585–3595.

Haam, J., Zhou, J., Cui, G., and Yakel, J.L. (2018). Septal cholinergic neurons gate hippocampal output to entorhinal cortex via oriens lacunosum moleculare interneurons. Proc. Natl. Acad. Sci. USA *115*, E1886–E1895.

Hasselmo, M.E. (2005). What is the function of hippocampal theta rhythm?–Linking behavioral data to phasic properties of field potential and unit recording data. Hippocampus *15*, 936–949.

Hernandez, C.M., Cortez, I., Gu, Z., Colón-Sáez, J.O., Lamb, P.W., Wakamiya, M., Yakel, J.L., and Dineley, K.T. (2014). Research tool: validation of floxed α7 nicotinic acetylcholine receptor conditional knockout mice using in vitro and in vivo approaches. J. Physiol. *592*, 3201–3214.

Hughes, R.N. (2004). The value of spontaneous alternation behavior (SAB) as a test of retention in pharmacological investigations of memory. Neurosci. Biobehav. Rev. *28*, 497–505.

Hummos, A., and Nair, S.S. (2017). An integrative model of the intrinsic hippocampal theta rhythm. PLoS ONE *12*, e0182648.

Igarashi, K.M. (2015). Plasticity in oscillatory coupling between hippocampus and cortex. Curr. Opin. Neurobiol. *35*, 163–168.

Jeewajee, A., Barry, C., O'Keefe, J., and Burgess, N. (2008a). Grid cells and theta as oscillatory interference: electrophysiological data from freely moving rats. Hippocampus *18*, 1175–1185.

Jeewajee, A., Lever, C., Burton, S., O'Keefe, J., and Burgess, N. (2008b). Environmental novelty is signaled by reduction of the hippocampal theta frequency. Hippocampus *18*, 340–348.

Ji, D., and Dani, J.A. (2000). Inhibition and disinhibition of pyramidal neurons by activation of nicotinic receptors on hippocampal interneurons. J. Neurophysiol. *83*, 2682–2690.

Ji, D., Lape, R., and Dani, J.A. (2001). Timing and location of nicotinic activity enhances or depresses hippocampal synaptic plasticity. Neuron *31*, 131–141.

Kellar, K.J., Martino, A.M., Hall, D.P., Jr., Schwartz, R.D., and Taylor, R.L. (1985). High-affinity binding of [3H]acetylcholine to muscarinic cholinergic receptors. J. Neurosci. *5*, 1577–1582.

Kenney, J.W., and Gould, T.J. (2008). Modulation of hippocampus-dependent learning and synaptic plasticity by nicotine. Mol. Neurobiol. *38*, 101–121.

Klausberger, T., Magill, P.J., Márton, L.F., Roberts, J.D., Cobden, P.M., Buzsáki, G., and Somogyi, P. (2003). Brain-state- and cell-type-specific firing of hippocampal interneurons in vivo. Nature *421*, 844–848.

Korotkova, T., Ponomarenko, A., Monaghan, C.K., Poulter, S.L., Cacucci, F., Wills, T., Hasselmo, M.E., and Lever, C. (2018). Reconciling the different faces of hippocampal theta: The role of theta oscillations in cognitive, emotional and innate behaviors. Neurosci. Biobehav. Rev. *85*, 65–80.

Kramis, R., Vanderwolf, C.H., and Bland, B.H. (1975). Two types of hippocampal rhythmical slow activity in both the rabbit and the rat: relations to behavior and effects of atropine, diethyl ether, urethane, and pentobarbital. Exp. Neurol. *49*, 58–85.

Lalonde, R. (2002). The neurobiological basis of spontaneous alternation. Neurosci. Biobehav. Rev. *26*, 91–104.

Lawson, V.H., and Bland, B.H. (1993). The role of the septohippocampal pathway in the regulation of hippocampal field activity and behavior: analysis by the intraseptal microinfusion of carbachol, atropine, and procaine. Exp. Neurol. *120*, 132–144.

Leão, R.N., Mikulovic, S., Leão, K.E., Munguba, H., Gezelius, H., Enjin, A., Patra, K., Eriksson, A., Loew, L.M., Tort, A.B., and Kullander, K. (2012). OLM interneurons differentially modulate CA3 and entorhinal inputs to hippocampal CA1 neurons. Nat. Neurosci. *15*, 1524–1530.

Lee, M.G., Chrobak, J.J., Sik, A., Wiley, R.G., and Buzsáki, G. (1994). Hippocampal theta activity following selective lesion of the septal cholinergic system. Neuroscience *62*, 1033–1047.

Leung, L.W., and Desborough, K.A. (1988). APV, an N-methyl-D-aspartate receptor antagonist, blocks the hippocampal theta rhythm in behaving rats. Brain Res. *463*, 148–152.

Leung, L.S., and Shen, B. (2004). Glutamatergic synaptic transmission participates in generating the hippocampal EEG. Hippocampus *14*, 510–525.

Levey, A.I., Edmunds, S.M., Koliatsos, V., Wiley, R.G., and Heilman, C.J. (1995). Expression of m1-m4 muscarinic acetylcholine receptor proteins in rat hippocampus and regulation by cholinergic innervation. J. Neurosci. *15*, 4077–4092.

Levin, E.D., and Simon, B.B. (1998). Nicotinic acetylcholine involvement in cognitive function in animals. Psychopharmacology (Berl.) *138*, 217–230.

Lovett-Barron, M., Turi, G.F., Kaifosh, P., Lee, P.H., Bolze, F., Sun, X.H., Nicoud, J.F., Zemelman, B.V., Sternson, S.M., and Losonczy, A. (2012). Regulation of neuronal input transformations by tunable dendritic inhibition. Nature Neurosci. *15*, 423–430, S421–S423.

Luikart, B.W., Nef, S., Virmani, T., Lush, M.E., Liu, Y., Kavalali, E.T., and Parada, L.F. (2005). TrkB has a cell-autonomous role in the establishment of hippocampal Schaffer collateral synapses. J. Neurosci. *25*, 3774–3786.

Martin, B.R., and Aceto, M.D. (1981). Nicotine binding sites and their localization in the central nervous system. Neurosci. Biobehav. Rev. *5*, 473–478.

Means, L.W., Leander, J.D., and Isaacson, R.L. (1971). The effects of hippocampectomy on alternation behavior and response of novelty. Physiol. Behav. *6*, 17–22.

Mikulovic, S., Restrepo, C.E., Hilscher, M.M., Kullander, K., and Leão, R.N. (2015). Novel markers for OLM interneurons in the hippocampus. Front. Cell. Neurosci. *9*, 201.

Mikulovic, S., Restrepo, C.E., Siwani, S., Bauer, P., Pupe, S., Tort, A.B.L., Kullander, K., and Leão, R.N. (2018). Ventral hippocampal OLM cells control type 2 theta oscillations and response to predator odor. Nat. Commun. *9*, 3638.

Monmaur, P., and Breton, P. (1991). Elicitation of hippocampal theta by intraseptal carbachol injection in freely moving rats. Brain Res. *544*, 150–155.

Monmaur, P., Ayadi, K., and Breton, P. (1993). Hippocampal EEG responses induced by carbachol and atropine infusions into the septum and the hippocampus in the urethane-anaesthetized rat. Brain Res. *631*, 317–324.

Neymotin, S.A., Hilscher, M.M., Moulin, T.C., Skolnick, Y., Lazarewicz, M.T., and Lytton, W.W. (2013). Ih tunes theta/gamma oscillations and cross-frequency coupling in an in silico CA3 model. PLoS ONE *8*, e76285.

Petsche, H., Gogolák, G., and Stumpf, C. (1968). Septal unit firing and the shape of theta waves in the rabbit's hippocampus. Electroencephalogr. Clin. Neurophysiol. *24*, 390.

Sainsbury, R.S., Heynen, A., and Montoya, C.P. (1987). Behavioral correlates of hippocampal type 2 theta in the rat. Physiol. Behav. *39*, 513–519.

Séguéla, P., Wadiche, J., Dineley-Miller, K., Dani, J.A., and Patrick, J.W. (1993). Molecular cloning, functional properties, and distribution of rat brain alpha 7: a nicotinic cation channel highly permeable to calcium. J. Neurosci. *13*, 596–604.

Siwani, S., Franca, A.S.C., Mikulovic, S., Reis, A., Hilscher, M.M., Edwards, S.J., Leao, R.N., Tort, A.B.L., and Kullander, K. (2018). OLMα2 cells bidirectionally modulate learning. Neuron *99*, 404–412 e403.

Stewart, M., and Fox, S.E. (1990). Do septal neurons pace the hippocampal theta rhythm? Trends Neurosci. *13*, 163–168.

Stumpf, C., Petsche, H., and Gogolak, G. (1962). The significance of the rabbit's septum as a relay station between the midbrain and the hippocampus. II. The differential influence of drugs upon both the septal cell firing pattern and the hippocampus theta activity. Electroencephalogr. Clin. Neurophysiol. *14*, 212–219.

Taniguchi, H., He, M., Wu, P., Kim, S., Paik, R., Sugino, K., Kvitsiani, D., Fu, Y., Lu, J., Lin, Y., et al. (2011). A resource of Cre driver lines for genetic targeting of GABAergic neurons in cerebral cortex. Neuron *71*, 995–1013.

Tsien, J.Z., Chen, D.F., Gerber, D., Tom, C., Mercer, E.H., Anderson, D.J., Mayford, M., Kandel, E.R., and Tonegawa, S. (1996). Subregion- and cell type-restricted gene knockout in mouse brain. Cell *87*, 1317–1326.

Vanderwolf, C.H., and Baker, G.B. (1986). Evidence that serotonin mediates non-cholinergic neocortical low voltage fast activity, non-cholinergic hippocampal rhythmical slow activity and contributes to intelligent behavior. Brain Res. *374*, 342–356.

Vanderwolf, C.H., Leung, L.W., and Cooley, R.K. (1985). Pathways through cingulate, neo- and entorhinal cortices mediate atropine-resistant hippocampal rhythmical slow activity. Brain Res. *347*, 58–73.

Wells, C.E., Amos, D.P., Jeewajee, A., Douchamps, V., Rodgers, J., O'Keefe, J., Burgess, N., and Lever, C. (2013). Novelty and anxiolytic drugs dissociate

two components of hippocampal theta in behaving rats. J. Neurosci. *33*, 8650–8667.

Whishaw, I.Q., and Vanderwolf, C.H. (1973). Hippocampal EEG and behavior: changes in amplitude and frequency of RSA (theta rhythm) associated with spontaneous and learned movement patterns in rats and cats. Behav. Biol. *8*, 461–484.

Winson, J. (1978). Loss of hippocampal theta rhythm results in spatial memory deficit in the rat. Science *201*, 160–163.

Witten, I.B., Lin, S.C., Brodsky, M., Prakash, R., Diester, I., Anikeeva, P., Gradinaru, V., Ramakrishnan, C., and Deisseroth, K. (2010). Cholinergic interneurons control local circuit activity and cocaine conditioning. Science *330*, 1677–1681.

Yakel, J.L. (2014). Nicotinic ACh receptors in the hippocampal circuit; functional expression and role in synaptic plasticity. J. Physiol. *592*, 4147–4153.

Yoder, R.M., and Pang, K.C. (2005). Involvement of GABAergic and cholinergic medial septal neurons in hippocampal theta rhythm. Hippocampus *15*, 381–392.

Please cite this article in press as: Gu et al., Hippocampal Interneuronal α7 nAChRs Modulate Theta Oscillations in Freely Moving Mice, Cell Reports (2020), https://doi.org/10.1016/j.celrep.2020.107740



## STAR★METHODS

### KEY RESOURCES TABLE

| REAGENT or RESOURCE | SOURCE | IDENTIFIER |
|---|---|---|
| Antibodies | | |
| Rabbit anti dsred antibody | Clonetech | Cat# 632496; RRID:AB_10013483 |
| biotinylated goat anti-rabbit secondary antibody | Vector Laboratories | Cat# BA-1000; RRID:AB_2313606 |
| Bacterial and Virus Strains | | |
| pAAV-EF1a-DIO- hChR2(H134R)-mCherry-WPRE-HGHpA | Witten et al., 2010 | addgene #20297 |
| pAAV-EF1a-DIO-mCherry-WPRE-HGHpA | Witten et al., 2010 | addgene #20299 |
| Chemicals, Peptides, and Recombinant Proteins | | |
| methyllycaconitine | Tocris | Cat# 1029 |
| dihydro-β-erythroidine | Tocris | Cat# 2349 |
| atropine | Sigma | Cat# A0132 |
| acetylcholine | Sigma | Cat# A6625 |
| choline | Sigma | Cat# C7527 |
| Critical Commercial Assays | | |
| BaseScope Duplex Detection Reagent kit | Advanced Cell Diagnostics | Cat# 323810 |
| RnaScope Duplex Detection Reagent kit | Advanced Cell Diagnostics | Cat# 322500 |
| Vectastain Elite ABC kit | Vector Laboratories | Cat# PK-6100 |
| DAB Peroxidase Substrate Kit | Vector Laboratories | Cat# SK-4100 |
| Experimental Models: Organisms/Strains | | |
| Mouse: floxed α7 nAChR (B6(Cg)-Chrna7tm1.1Ehs/YakelJ) | The Jackson Laboratory | Cat# 026965 |
| Mouse: Gad2-cre (B6N.Cg-Gad2tm2(cre) Zjh/J) | The Jackson Laboratory | Cat# 019022 |
| Mouse: CaMK2a-cre (B6.Cg-Tg(Camk2a-cre)T29-1Stl/J) | The Jackson Laboratory | Cat# 005359 |
| Mouse: ChAT-cre (B6;129S6-Chattm2(cre) Lowl/J) | The Jackson Laboratory | Cat# 006410 |
| Mouse: Sst-cre (Sst tm2.1(cre)Zjh) | The Jackson Laboratory | Cat# 013044 |
| Mouse: Rosa tdTomato (B6.Cg-Gt(ROSA) 26Sor tm14(CAG-tdTomato)Hze/J) | The Jackson Laboratory | Cat# 007914 |
| Mouse: OLMα2-cre mice (Tg(Chrna2cre) OE29Gsat/Mmucd) | Mutant Mouse Resource and Research Centers | Cat# 036704-UCD |
| Oligonucleotides | | |
| α7 nAChR mRNA probe | Advanced Cell Diagnostics | Cat# 724751-C2 |
| Sst mRNA probe | Advanced Cell Diagnostics | Cat# 712861 |
| GAD2 mRNA probe | Advanced Cell Diagnostics | Cat# 714361 |
| CaMK2a mRNA probe | Advanced Cell Diagnostics | Cat# 724771 |
| α2 nAChR mRNA probe | Advanced Cell Diagnostics | Cat# 416881 |
| Software and Algorithms | | |
| NeuroExplorer | Nex Technologies | https://www.neuroexplorer.com/ |
| EthoVision | Noldus | https://www.noldus.com/ethovision-xt |
| Cerebus acquisition system | Blackrock Microsystems | https://www.blackrockmicro.com/neuroscience-research-products/neural-data-acquisition-systems/cerebus-daq-system/ |

(*Continued on next page*)

*Continued*

| REAGENT or RESOURCE | SOURCE | IDENTIFIER |
|---|---|---|
| pClamp | Molecular Devices | https://www.moleculardevices.com/products/axon-patch-clamp-system/acquisition-and-analysis-software/pclamp-software-suite#gref |

## RESOURCE AVAILABILITY

### Lead Contact

Further information and requests for resources and reagents should be directed to and will be fulfilled by the Lead Contact, Jerrel Yakel (yakel@niehs.nih.gov).

### Materials Availability

This study did not generate new unique reagents.

### Data and Code Availability

This study did not generate any unique datasets or code.

## EXPERIMENTAL MODEL AND SUBJECT DETAILS

Wild-type C57BL/6 mice, floxed α7 nAChR knockout mice (B6(Cg)-Chrna7tm1.1Ehs/YakelJ), Gad2-cre (B6N.Cg-Gad2tm2(cre)Zjh/J), CaMK2a-cre (B6.Cg-Tg(Camk2a-cre)T29-1Stl/J), ChAT-cre (B6;129S6-Chattm2(cre)Lowl/J), Sst-cre (Ssttm2.1(cre)Zjh), and Rosa tdTomato (B6.Cg-Gt(ROSA)26Sortm14(CAG-tdTomato)Hze/J) transgenic mice were originally purchased from Jackson Laboratory and then bred at NIEHS. OLMα2-cre mice (Tg(Chrna2cre)OE29Gsat/Mmucd) were originally obtained from Mutant Mouse Resource and Research Centers (MMRRC) and then bred at NIEHS. Male mice (4-5 month old) were used for experiments. All mice were housed under normal light/dark cycle. All procedures were approved and performed in compliance with NIEHS/NIH Humane Care and Use of Animals in Research protocols.

## METHOD DETAILS

### Materials

Selective nAChR subtype antagonists were from Tocris or Sigma. Unless otherwise indicated, general chemicals for slice culture were obtained from Sigma or Invitrogen. AAV serotype 9 helper plasmid was obtained from James Wilson at the University of Pennsylvania. The AAV vector with floxed ChR2 (Addgene #20297) plasmid was obtained from Karl Deisseroth (Witten et al., 2010). AAV viruses were packaged with serotype 9 helper at the Viral Vector Core facility at NIEHS.

### Intracranial electrode and cannula implantation

The procedures were the same as described before (Gu et al., 2017). To study the effects of cholinergic receptor antagonists on hippocampal theta oscillations *in vivo*, wild-type male mice (4-5 months old) underwent intracranial electrode and cannula implantation using sterile surgical techniques. Mice were anaesthetized with ketamine (100 mg/kg) and xylazine (7 mg/kg) and placed in a stereotaxic device. Cannula-electrode combos, with the guide cannula (Gauge 26, from Plastics One) surrounded by 4 polyimide-coated 50-μm stainless steel recording wires were implanted into hippocampal area CA1 (−2.3 mm anteroposterior, 2.0 mm mediolateral, and 1.80 mm dorsoventral from bregma). Each mouse only receives one cannula-electrode combo implantation and thus the infusions are unilateral. The wires were connected to a printed circuit board (San Francisco Circuits) and miniature Omnetics connector. Implanted electrodes were secured with dental acrylic. To compare theta oscillations among different subpopulation α7 nAChR knockout mice, male mice (4-5 months old) underwent the same surgical procedures as described above, but only with intracranial electrode (without cannula) implantation. A bundle of 4 polyimide-coated 50-μm stainless steel recording wires (connected to Omnetics connectors, made by Microprobes) were implanted into dorsal CA1 area (−2.3 mm anteroposterior, 2.0 mm mediolateral, and 1.80 mm dorsoventral from bregma). Mice were singly housed following surgery and were allowed to recover from surgery for at least 1 week before any further experiments.

### In vivo electrophysiological data acquisition and drug infusion

During *in vivo* hippocampal electrophysiological recordings, mice were placed in a custom-built open-top dark arena as desbribed before (Gu et al., 2017). An overhead camera was used to record the behaviors for later offline analyses. Mice were habituated by being exposed to the arena for 10 min/day for 3 days before recordings were begun. Neural activities were transmitted via a wireless

headstage (Triangle BioSystems International) and were acquired with the Cerebus acquisition system (Blackrock Microsystems). Theta oscillations were analyzed with NeuroExplorer software (Nex Technologies).

On the day of electrophysiological recordings, while the mice were under isoflurane anesthesia (1.5% Isoflurane in oxygen), an internal infusion cannula was inserted into the guide cannula (that was previously implanted) to deliver 0.5 μL of either saline, the α7 nAChR antagonist MLA (0.2 μM), the α4β2 nAChR antagonist DHβE (0.1 mM), or a mix of atropine (0.1 mM), MLA (0.2 μM), and DHβE (0.1 mM), at a rate of 0.1 μl/min. On completion of the infusion, a wireless headstage was plugged into the connector that was previously implanted. Mice were then returned to home cages and allowed to recover for 10 min from isoflurane anesthesia and then placed into the open field arena for continuous recordings for 10 min. Each mouse underwent the same infusion and recording procedure multiple times for different antagonist infusion, with at least 3 rest days between each infusion treatment. The order of treatment presentation was randomized among mice.

For *in vivo* hippocampal electrophysiological recordings from different subpopulation α7 nAChR knockout mice, mice underwent a brief isoflurane anesthesia to plug the wireless headstage into the connector. Recordings were carried out after a 10 min recovery from isoflurane anesthesia.

### Y-maze spontaneous alternation test

Spatial working memory was examined with Y-maze (Med Associates) spontaneous alternation test as describe before (Gu et al., 2017). For the experiments with drug infusion, the mice were infused with antagonists under isoflurane, allowed to recover for 10 min in home cage and then put in the Y-maze to run freely for 8 min. One antagonist infusion and Y-maze exploration session was done per day per mouse. Each mouse underwent the same infusion and Y-maze procedure multiple times, being treated with each of the antagonists with at least 3 rest days between treatments. The environment and floor bedding materials were changed during each test. The order of treatment presentation was randomized among mice. For the experiments with α7 nAChR knockout in different neuronal subpopulations, mice were directly put into the Y-maze to run for 8 min. Locomotion was recorded with an overhead camera and later analyzed offline with Ethovision (Noldus) to calculate the alternation rate. The alternation score (%) was calculated as (the number of three successive arm choices that include one of each arm) / (total arm entries - 2) × 100. An arm entry was counted when all four limbs were within an arm.

### In vitro septo-entorhinal-hippocampal slice tri-culture preparation and theta induction

Theta-like oscillations were induced *in vitro* in septo-entorhinal-hippocampal slice tri-culture preparations by pairing cholinergic activation with Shaffer collateral activation, as previously described (Gu and Yakel, 2017). For the slice preparation, we had to include the entorhinal cortex to induce theta-like oscillations (Gu and Yakel, 2017). This dictates the use of ventral (but not dorsal) hippocampus that is connected to the entorhinal cortex. Briefly, horizontal entorhino-hippocampal slices (350 μm) from wild-type mice (6 to 8 days old) and coronal septal slices from ChAT-cre mice were cut with a vibratome (Leica, VT1000S) to dissect out the EC-containing hippocampus slice and medial septal tissue, respectively. These two parts were then placed next to each other on a 6-well polyester Transwell insert (Corning) and cultured there for about 3 weeks before being used for experiments. Cholinergic terminals in the hippocampus were optogenetically activated through ChR2 that was selectively expressed in ChAT-cre expressing (cholinergic) neurons. ChR2 was activated with 488-nm light (20 ms) through a 40 × objective with an Andor spinning disk confocal microscope (Andor technology). The Schaffer collateral pathway was activated through a stimulating electrode placed in the stratum radiatum through a stimulator (Grass S88X). The stimulation intensity was 1-10 μA for 0.1 ms.

### Field potential and whole-cell patch clamp recordings in vitro

*In vitro* electrophysiological recordings were performed as described before (Gu and Yakel, 2011, 2017). Briefly, 3 weeks after *in vitro* culturing, the co-cultured slices were removed from the inserts and put into a submerged chamber, continuously perfused with 95% $O_2$/5%$CO_2$ balanced ACSF (in mM, 122 NaCl, 2.5 KCl, 2 $MgCl_2$, 2 $CaCl_2$, 1.2 $NaH_2PO_4$, 25 $NaHCO_3$, 25 glucose) at a rate of 1 ml/min. Theta-like oscillations were recorded as local field potentials in hippocampal CA1 stratum lacunosum moleculare through a glass pipette filled with ACSF. EPSCs were recorded at −60 mV under voltage clamp through a glass pipette filled with internal solution (in mM, 130 potassium gluconate, 2 $MgCl_2$, 3 MgATP, 0.3 $Na_2GTP$, 10 KCl, 10 HEPES, and 1 EGTA, with pH ~7.2-7.3 and osmolarity ~280-290 mOsm). Field potential and whole cell patch clamp recordings were performed with Multiclamp 700B amplifier (Axon Instruments). Data were digitized with Digidata 1550, collected with Clampex and analyzed with Clampfit (Axon Instruments). MLA (10 nM) or DHβE (10 μM) was bath applied 5 min before, during, and after cholinergic pairing. ACh was locally perfused to CA1 area through a glass pipette with a Picospritzer (10 psi) for 1 s immediately before SC stimulation.

### Choline-induced α7 nAChR current in cultured hippocampal slices

Hippocampal slices were from GAD2-cre, Sst-cre, CaMKII-cre, and OLMα2-cre mice with or without being crossed with floxed α7 nAChR mice. Cre-positive neurons were visualized by Cre-dependent mCherry expression through AAV viral infection. The AAV viruses were delivered to the slices 1 day after culture. The cultured slices were used 3 weeks after viral infection for either fluorescent microscopy imaging after counter-staining with DAPI, or for choline-induced α7 nAChR current recording. α7 nAChR-mediated currents were recorded with whole cell patch clamp, and induced by pressure applications (50 ms, 10 psi) of 10 mM choline (Hernandez et al., 2014) at 2 min intervals through a glass pipette placed next to the cells under recording (about 50 μm away from the soma).

Please cite this article in press as: Gu et al., Hippocampal Interneuronal α7 nAChRs Modulate Theta Oscillations in Freely Moving Mice, Cell Reports (2020), https://doi.org/10.1016/j.celrep.2020.107740



Pressure was applied through a PPM-2 pneumatic pump (Harvard Apparatus). TTX (tetrodotoxin, 1 μm) was added to the perfusion ACSF and choline solution. Whole cell patch clamp was performed the same way as in recording EPSCs described above. Cre-positive (mCherry expressing) neurons were visualized with 560 nm laser light. Choline-induced α7 nAChR currents were recorded in neurons located in hippocampal CA1 area.

### In situ hybridization

Adult GAD-α7KO, CaMK2a-α7KO, Sst-α7KO, OLMα2-α7KO and OLMα2-α7KO; R/C::tdTomato mice and littermate controls, n = 3 males per strain, were anesthetized with phenobarbital and transcardially perfused with 0.1 M phosphate-buffered saline (PBS) followed by 4% paraformaldehyde (PFA) in PBS. Brains were removed from the skull and postfixed overnight in 4% PFA at 4°C. Following rinse in PBS, brains were cryoprotected in 30% sucrose in PBS and embedded in tissue-freezing medium (TFM-5, Triangle Biomedical Sciences). 14 μm coronal cryosections of septum and dorsal hippocampus were collected onto slides and every eighth section was processed for mRNA or immunolabeling. *In situ* hybridization was performed on GAD-α7KO, CaMK2a-α7KO, Sst-α7KO, and OLMα2-α7KO tissue using BaseScope probes (Advanced Cell Diagnostics, Newark, CA) for α7 nAChR (BA-Mm-Chrna7-2zz-st-C2; 724751-C2) and Sst (BA-Mm-Sst-E1E2; 712861), GAD2 (BA-Mm-Gad2-E1E2; 714361), or CaMK2a (BA-Mm-Camk2a-3EJ; 724771) according to the manufacturer's instructions for the BaseScope Duplex protocol. Tissue was counterstained with Gill's Hematoxylin #1 (24242-1000, Polysciences, Inc., Warrington, PA) For OLMα2-α7KO;R/C::tdTomato tissue, *in situ* hybridization was performed on using RnaScope probe α2 nAChR (Mm-Chrna2; 416881) or BaseScope probe for α7 nAChR, followed by immunohistochemistry using Rabbit anti dsred primary antibody (1:1000; Clonetech; 632496) and biotinylated goat anti-rabbit secondary antibody (1:500; Vector Laboratories; BA-1000). Immunoreactivity was detected with the Vectastain Elite ABC kit (Vector Laboratories; PK-6100) and DAB Peroxidase Substrate Kit (Vector Laboratories; SK-4100). All slides were coverslipped with Vectamount permanent mounting medium (H-5000, Vector Laboratories Inc.). Images were collected on an automated Zeiss epifluorescent microscope.

## QUANTIFICATION AND STATISTICAL ANALYSIS

Theta oscillations were analyzed with NeuroExplorer software as described before (Gu et al., 2017). For *in vivo* recordings, the spectrogram analysis was performed with 1 s sliding analysis window. The power spectral density for a trial was calculated by averaging these 1 s bins while the animal was engaged in active movements (defined as running at a speed above 2 cm/s; a speed below 1.5 cm/s is defined as immobile) that lasted for at least 10 s, excluding the first episode when animal was just placed in the arena. To compare the effects of intracranial antagonist infusion on hippocampal theta power, the peak theta power in the 6-12 Hz range was measured during running after antagonist or vehicle infusion and compared with RM one-way ANOVA of matched or repeated-measures in GraphPad Prism 7, followed by Dunnett's multiple comparisons test to compare with saline group. To compare theta strength in mice with α7 receptor knockout in different neuronal subpopulations, due to large variation of baseline recordings among individual mice, the peak theta power during active exploration was first normalized to the averaged power at the same frequency during immobility from the same animal and then compared between animals. The averaged power during immobility was calculated by averaging the 1 s bins while the animal was immobile for at least 10 s. For *in vitro* recordings, the theta power for an individual trace was analyzed (with 0.1 s sliding window) for the 1 s period following the SC stimulation. The theta power for an individual slice was obtained by averaging peak power that measured from 5 consecutive traces at time points indicated in the figures. For whole cell recordings, the amplitudes of SC stimulation-induced synaptic responses were analyzed with Clampfit and graphs were made in Excel. The amplitudes were normalized to the mean of the 10 min baseline recording before cholinergic pairing. Values were presented as mean ± s.e.m. Treatment groups were compared with control group with non-matching ordinary one-way ANOVAs, followed by Dunnett's multiple comparisons test, unless otherwise specifically stated.